JCB Article

SCAR is a primary regulator of Arp2/3-dependent morphological events in *Drosophila*

Jennifer A. Zallen,[1,2] Yehudit Cohen,[1] Andrew M. Hudson,[3] Lynn Cooley,[3] Eric Wieschaus,[2] and Eyal D. Schejter[1]

[1]Department of Molecular Genetics, Weizmann Institute of Science, Rehovot 76100, Israel
[2]Howard Hughes Medical Institute, Department of Molecular Biology, Princeton University, Princeton, NJ 08544
[3]Department of Genetics, Yale University Medical School, New Haven, CT 06520

The Arp2/3 complex and its activators, Scar/WAVE and Wiskott-Aldrich Syndrome protein (WASp), promote actin polymerization in vitro and have been proposed to influence cell shape and motility in vivo. We demonstrate that the *Drosophila* Scar homologue, SCAR, localizes to actin-rich structures and is required for normal cell morphology in multiple cell types throughout development. In particular, SCAR function is essential for cytoplasmic organization in the blastoderm, axon development in the central nervous system, egg chamber structure during oogenesis, and adult eye morphology. Highly similar developmental requirements are found for subunits of the Arp2/3 complex. In the blastoderm, SCAR and Arp2/3 mutations result in a reduction in the amount of cortical filamentous actin and the disruption of dynamically regulated actin structures. Remarkably, the single *Drosophila* WASp homologue, Wasp, is largely dispensable for these numerous Arp2/3-dependent functions, whereas SCAR does not contribute to cell fate decisions in which Wasp and Arp2/3 play an essential role. These results identify SCAR as a major component of Arp2/3-dependent cell morphology during *Drosophila* development and demonstrate that the Arp2/3 complex can govern distinct cell biological events in response to SCAR and Wasp regulation.

Introduction

The spatially regulated polymerization of actin monomers into filaments provides a widely used mechanism underlying cell morphology and motility. During cell migration and axon extension, localized actin filament assembly occurs at the advancing cell surface (Borisy and Svitkina, 2000). Through a related mechanism, actin polymerization propels the movement of intracellular pathogens within host cytoplasm (Dramsi and Cossart, 1998). Actin polymerization is also required in nonmotile cells for cytoplasmic organelle transport, endocytosis, and the organization of dynamic actin structures (Winter et al., 1997, 1999; Qualmann et al., 2000; Pelham and Chang, 2001; Taunton, 2001).

Biochemical studies have provided detailed information about the molecules that influence actin dynamics (Pantaloni et al., 2001). Of particular significance is the Arp2/3 complex that stimulates microfilament nucleation, the rate-limiting step in actin polymerization (Mullins et al., 1998; Welch et al., 1998). The Arp2/3 complex consists of seven protein subunits, including the actin-related Arp2 and Arp3, and is conserved among eukaryotes (Machesky and Gould, 1999; May, 2001). Members of the evolutionarily conserved Wiskott-Aldrich Syndrome protein (WASp)* and Scar/WAVE family function as strong potentiators of Arp2/3 complex activity (Higgs and Pollard, 2001). Distinct WASp and Scar/WAVE branches of this family have been recognized in diverse organisms, including *Dictyostelium*, *Caenorhabditis elegans*, *Drosophila*, and mammals. WASp and Scar/WAVE proteins share a common domain structure that mediates activation of the Arp2/3 complex in response to multiple signaling pathways. All members of the WASp-Scar/WAVE family possess a common COOH-terminal (WA) domain that stimulates actin polymerization through association with monomeric actin and the Arp2/3 complex, whereas their NH_2-terminal domains are structurally distinct and serve as signal-responsive regulatory regions (Fig. 1). The molecular mechanisms controlling WASp function are well characterized (Fawcett and Pawson, 2000), whereas regulatory aspects of Scar function are now beginning to emerge (Takenawa and Miki, 2001).

The single WASp/Scar protein in budding yeast is required for processes that have been shown to be Arp2/3 dependent (Li, 1997; Naqvi et al., 1998), indicating a functional

Address correspondence to Eyal D. Schejter, Dept. of Molecular Genetics, Weizmann Institute of Science, Rehovot 76100, Israel. Tel.: 972-8-934-2207. Fax: 972-8-934-4108. E-mail: eyal.schejter@weizmann.ac.il

Key words: Scar; Arp2/3; Wasp; actin; *Drosophila*

*Abbreviation used in this paper: WASp, Wiskott-Aldrich Syndrome protein.

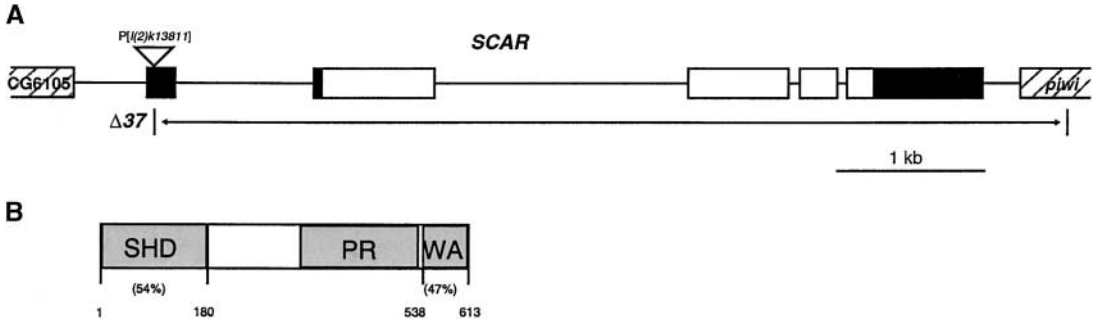

Figure 1. **Molecular genetics of *SCAR*.** (A) Genomic organization of the *SCAR* transcription unit. Boxes represent exons, and lines represent introns. The 253 nucleotide 5′ UTR and the 730 nucleotide longest 3′ UTR are shaded black. The site of the P-element insertion *l(2)k13811* within the first exon and the extent of the *Δ37* excision are indicated. Hatched boxes mark the ORFs of neighboring transcription units CG6105 and *piwi*. (B) Domain structure of *Drosophila* SCAR. This includes the regulatory SCAR homology domain (SHD), unique to this protein family, a proline-rich region (PR), and the COOH-terminal actin/Arp2/3-interacting WA domain shared by all WASp/Scar proteins. Amino acid residue numbers at domain boundaries and sequence homology percentages between *Drosophila* SCAR and human Scar/WAVE-1 are indicated. (C) Alignment of Scar protein sequences from *Dictyostelium* (Dict Scar), *C. elegans* (Ce Scar), *Drosophila* (Dm SCAR), and human (hScar/WAVE 1, 2, and 3). Homologies are boxed, and identities are boxed and shaded. The *SCAR* transcript was defined by sequencing of the LP11386, SD10808, and SD02991 ESTs (Rubin et al., 2000). LP11386 differs at amino acids L^{194} and S^{195}. The *SCAR* transcript is described in the GadFly Genome Annotation Database (CG4636) and sequence data is available from GenBank/EMBL/DDBJ under accession no. AF247763.

connection in vivo as well as in vitro. In what cellular contexts does this system operate during development of multicellular organisms? Are the distinct WASp and Scar homologs present in such organisms involved in common or separate Arp2/3-dependent processes? Here, we describe the first mutant alleles of the single *Drosophila* Scar/WAVE homologue, *SCAR*, and compare its functions to those of the previously identified WASp homologue, *Wasp* (*Wsp*) (Ben-Yaacov et al., 2001). *SCAR* and *Wsp* appear to represent the only homologs of their respective subfamilies in the *Drosophila* genome, providing an opportunity to compare the functional requirements for these two major branches of the WASp/Scar protein family. Furthermore, the in vivo relevance of WASp and Scar to Arp2/3 complex functions during development of a multicellular organism can be assessed using mutant alleles in components of the *Drosophila* Arp2/3 complex (Hudson and Cooley, 2002). Our results suggest that Wasp and SCAR mediate distinct subsets of Arp2/3-dependent processes during *Drosophila* development. Although Wasp is required specifically for proper execution of asymmetric cell divisions in neural lineages, SCAR plays a major role in the Arp2/3 complex-dependent regulation of cell morphology.

Results

Drosophila SCAR colocalizes with actin structures during embryonic development

A search of the sequenced *Drosophila* genome identified a single Scar/WAVE homologue (*SCAR*, corresponding to transcription unit CG4636) that maps to cytogenetic band 32C4-5 on the second chromosome. We determined the structure of the *SCAR* transcript by sequencing three ESTs from the Berkeley *Drosophila* Genome Project database (Fig. 1). The 2,184 nucleotide *SCAR* transcript is predicted to encode a 613 amino acid protein possessing the major hallmarks of Scar/WAVE proteins (Fig. 1, B and C).

To examine SCAR protein expression and subcellular localization, we generated a polyclonal antibody to the unique SCAR NH_2-terminal domain (see Materials and methods). We found that SCAR protein is present in early blastoderm embryos and in the embryonic CNS (Fig. 2) consistent with its mRNA expression (unpublished data). In the blastoderm, SCAR protein colocalizes with filamentous actin structures that are dynamically regulated during the cell cycle (Fig. 2, A and C; see below). In the CNS, SCAR protein is specifically localized to axons (Fig. 2, E and F). This pattern of *SCAR* protein expression in the embryo provided us with an initial indication of the potential sites of *SCAR* gene activity.

Isolation of mutations in the *Drosophila SCAR* gene

To investigate SCAR function, two mutant alleles of *SCAR* were identified and characterized. The recessive lethal P-element insertion mutation *l(2)k13811* (Spradling et al., 1999) lies within the 5′ UTR of the *SCAR* transcript, 208 nucleotides upstream of the translation start codon (Fig. 1 A) (Berkeley *Drosophila* Genome Project; unpublished data). Chromosomes bearing precise excisions of this insertion complemented the lethality of *l(2)k13811* and were homozygous viable. In addition, ubiquitous expression of a full-length *SCAR* cDNA rescued the lethality of the *l(2)k13811* insertion. These data demonstrate that the zygotic recessive lethality is due to disruption of the *SCAR* gene by the *l(2)k13811* insertion, and we refer to this allele as $SCAR^{k13811}$. Moreover, embryos that are maternally and zygotically mutant for the $SCAR^{k13811}$ allele display a strong reduction in staining with the anti-SCAR antibody (Fig. 2, B and D), confirming that this insertion disrupts *SCAR* expression.

To obtain deletions in the *SCAR* locus, we generated imprecise excision alleles of the $SCAR^{k13811}$ insertion, all of which were homozygous lethal and failed to complement the lethality of $SCAR^{k13811}$. The homozygous lethality of the *Δ37* excision allele was rescued by ubiquitous expression of the full-length *SCAR* cDNA, and we refer to this allele as $SCAR^{\Delta 37}$. $SCAR^{\Delta 37}$ was molecularly characterized and removes all *SCAR* sequences downstream of the insertion site (Fig. 1 A). This excision event also removes portions of the neighboring *piwi* transcription unit. Since *piwi*

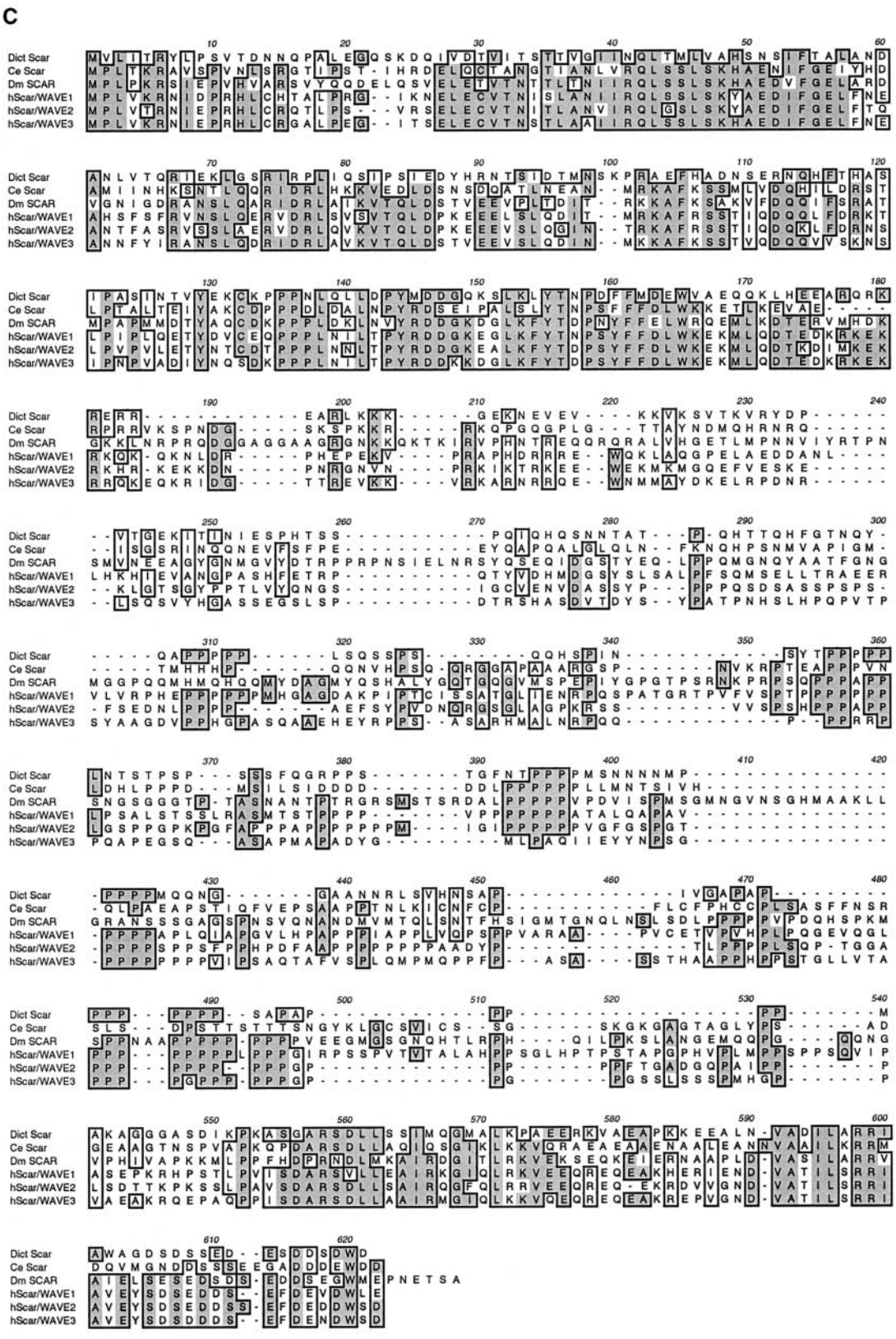

Figure 1 (continued)

function is restricted to maintenance and proliferation of germline stem cells (Cox et al., 1998, 2000), the $SCAR^{\Delta 37}$ phenotypes described below, in distinct tissues, are likely to represent consequences of disrupting *SCAR* function alone. Developmental defects were considerably weaker in $SCAR^{k13811}$, indicating that the insertion allele retains partial *SCAR* activity.

In addition to SCAR and Wasp (Ben-Yaacov et al., 2001), the sequenced *Drosophila* genome contains predicted homologs of the seven members of the Arp2/3

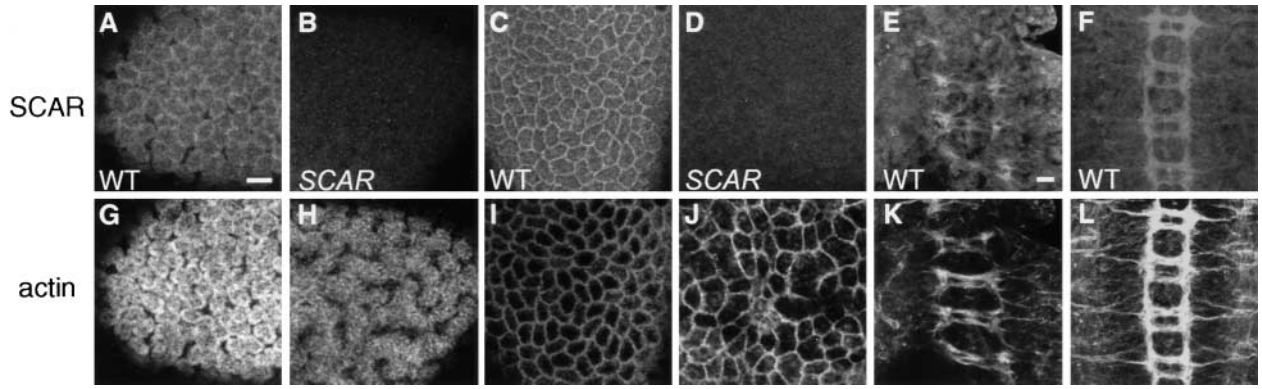

Figure 2. **SCAR protein expression in embryos.** Anti-SCAR polyclonal antibody (top row); filamentous actin labeled with phalloidin (bottom row). In wild-type embryos at cycle 12, SCAR protein colocalizes with actin in interphase (A, SCAR; G, actin) and metaphase (C, SCAR; I, actin). SCAR staining is reduced in cycle 12 *SCAR*^{mat} mutant embryos at interphase (B) or metaphase (D), indicating that this antibody detects SCAR protein. *SCAR*^{mat} blastoderm embryos were stained in the same tube as wild-type control embryos from *oskar*^{166} mutant mothers, identified by the absence of pole cells (Lehmann and Nusslein-Volhard, 1986). Note that actin structures appear disrupted in *SCAR* mutants (J); these defects are discussed below. In wild-type Oregon R embryos at stage 13, SCAR protein is enriched in growing axons (E) that also stain for filamentous actin (K). SCAR protein persists in later CNS axons (F) costained with actin (L). Bars, 10 μm.

complex (Fyrberg et al., 1994; Goldstein and Gunawardena, 2000). Mutations have been recovered in two Arp2/3 complex components, Arp3 (Rørth, 1996; Berkeley *Drosophila* Genome Project) and Arpc1 (Hudson and Cooley, 2002). This set of mutations provides an opportunity to analyze the role of Arp2/3-based signaling in different contexts within a multicellular organism and to ascertain the physiological contributions of the SCAR and Wasp activators.

SCAR and Arpc1 are required for cytoplasmic organization in the blastoderm embryo

Homozygous mutations in either *SCAR* allele result in zygotic lethality, which can occur during late embryogenesis, larval, and early pupal stages. However, maternally provided *SCAR* gene products may compensate for loss of zygotic gene function and mask an essential requirement during embryogenesis. To interfere with the maternal gene contribution, we used FLP-mediated recombination to produce

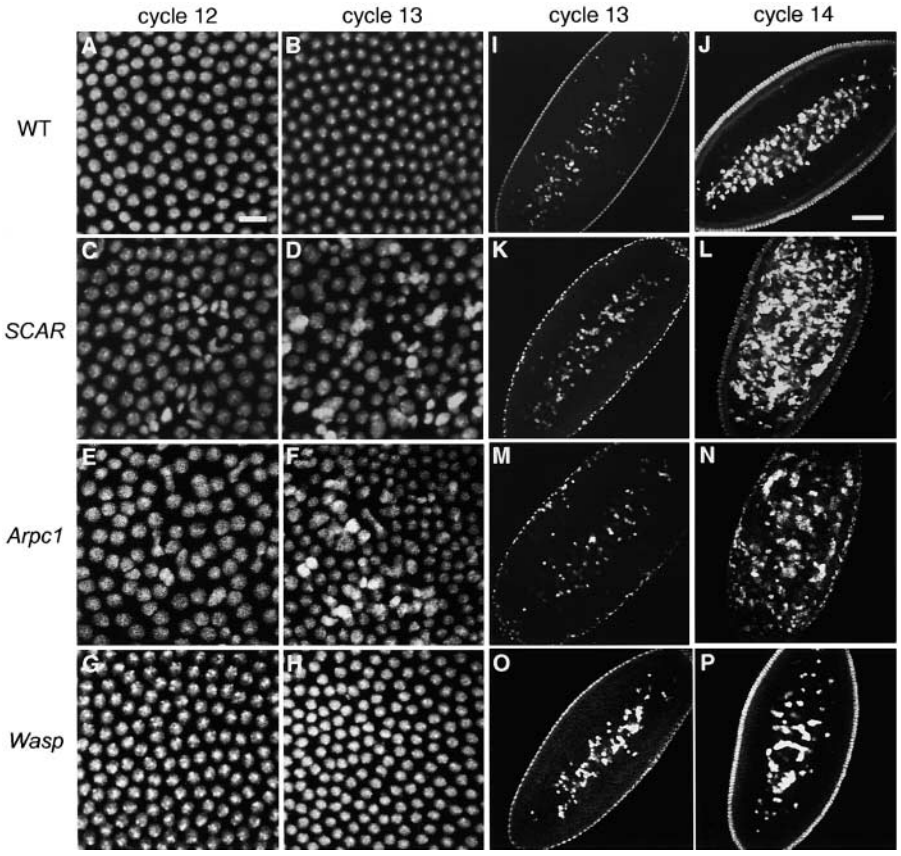

Figure 3. **Defects in nuclear arrangement and morphology in *SCAR* and *Arpc1* mutant embryos.** (A–H) Surface views of syncytial embryos. Cortical nuclei are uniformly distributed in wild-type cycle 12 (A) and 13 (B) embryos. Nuclei exhibit abnormal spacing and morphology in *SCAR*^{mat} cycle 12 (C) and 13 (D) embryos. Similar defects occur in *Arpc1*^{mat} cycle 12 (E) and 13 (F) embryos. *Wsp*^{mat} cycle 12 (G) and 13 (H) embryos have wild-type nuclear spacing. (I–P) Cross-sections of syncytial embryos. Wild-type embryos at cycle 13 (I) and 14 (J) exhibit a uniform layer of surface nuclei and a subset of central yolk nuclei. In *SCAR*^{mat} embryos, nuclei occasionally recede from the surface at cycle 13 (K) with a dramatic internal accumulation of nuclei by cycle 14 (L). *Arpc1*^{mat} embryos display mild nuclear disruption at cycle 13 (M) and severe internal accumulation of nuclei by cycle 14 (N). In contrast, *Wsp*^{mat} cycle 13 (O) and 14 (P) embryos exhibit wild-type nuclear arrangement. Bars: (A–H) 10 μm; (I–P) 50 μm.

homozygous mutant clones within the germline of heterozygous females (Chou and Perrimon, 1996). Strong disruption of maternal *SCAR* or *Arpc1* in this manner results in developmental arrest during oogenesis (see below). However, germline clones homozygous for the weaker $SCAR^{k13811}$ or $Arpc1^{R337st}$ alleles give rise to fertilizable eggs, enabling study of functional requirements for SCAR and the Arp2/3 complex during embryogenesis. These embryos are designated $SCAR^{mat}$ and $Arpc1^{mat}$, respectively. To compare the roles of SCAR and Wasp, we examined embryos derived from germline clones for the strong loss of function Wsp^{3} allele (Wsp^{mat} embryos). The Wsp^{3} frameshift mutation truncates the protein before the highly conserved WA domain that is required for Arp2/3 activation and is a probable null allele (Ben-Yaacov et al., 2001).

The early blastoderm embryo undergoes 13 nuclear divisions without accompanying cytokinesis, producing a multinucleate syncytium. The majority of nuclei migrate to the surface by cycle 10, where they undergo four synchronous rounds of division before their compartmentalization into individual cells during interphase of cycle 14 (Zalokar and Erk, 1976). Surface nuclei maintain a uniform distribution throughout these final syncytial divisions (Fig. 3, A and B). Examination of the spatial distribution of nuclei revealed a requirement for SCAR and Arpc1, but not Wasp, during these cortical division cycles (Fig. 3, C–H). $SCAR^{mat}$ and $Arpc1^{mat}$ mutants exhibited defects in the uniform spacing of interphase nuclei beginning in cycle 11, whereas Wsp^{mat} mutants displayed wild-type nuclear organization. By cycles 12 and 13, increased defects in nuclear spacing in *SCAR* and *Arpc1* were accompanied by the appearance of abnormal nuclear morphologies, including large or elongate DNA masses that are likely to represent the fusion of adjacent nuclei.

In wild-type syncytial embryos, nuclei are maintained in two separate populations: a uniform layer of surface nuclei and an internal mass of yolk nuclei. In $SCAR^{mat}$ and $Arpc1^{mat}$ embryos, displacement of surface nuclei into the interior was first observed at cycle 12 and increased in severity by cycle 14 (Fig. 3, L and N) (96% of cycle 14 $SCAR^{mat}$ embryos, $n = 24$; 100% of cycle 14 $Arpc1^{mat}$ embryos, $n = 24$). The severity of these defects was strongly correlated with increased division cycles, demonstrating a late onset progressive defect (for $SCAR^{mat}$ $p = 10^{-17}$, $n = 76$ embryos, and $r_{sp} = 0.80$; for $Arpc1^{mat}$ $p = 10^{-21}$, $n = 69$ embryos, and $r_{sp} = 0.87$; r_{sp} is the Spearman rank correlation coefficient). Nuclear displacement was rarely observed in wild-type and Wsp^{mat} embryos (Fig. 3, J and P) (3% of cycle 14 wild-type embryos, $n = 33$; 0% of cycle 14 Wsp^{mat} embryos, $n = 32$).

SCAR and Arpc1 are required for actin polymerization and regulation of dynamic actin structures in the blastoderm embryo

The syncytial blastoderm contains well-defined filamentous actin structures that exhibit dynamic cell cycle regulation (Karr and Alberts, 1986). Actin is organized into caps overlying individual nuclei during interphase of cortical cycles 10–14 (Fig. 4, A and C). During mitosis, actin is redistributed into a network of metaphase furrows that separate adjacent spindles (Fig. 5, A and C). Genetic and drug interference studies demonstrate that organization of the actin cytoskeleton is crucial for the uniform arrangement of blastoderm nuclei (Foe et al., 1993; Schejter and Wieschaus, 1993). The nuclear defects in *SCAR* mutants, and SCAR protein colocalization with filamentous actin (Fig. 2), raise the possibility that SCAR may function in the regulation of actin structures in the blastoderm embryo.

In $SCAR^{mat}$ embryos, actin caps appeared largely intact during interphase, although some defects were observed. In particular, $SCAR^{mat}$ actin caps were consistently smaller and less rounded than in wild type (Fig. 4 E, 22/35 embryos). In

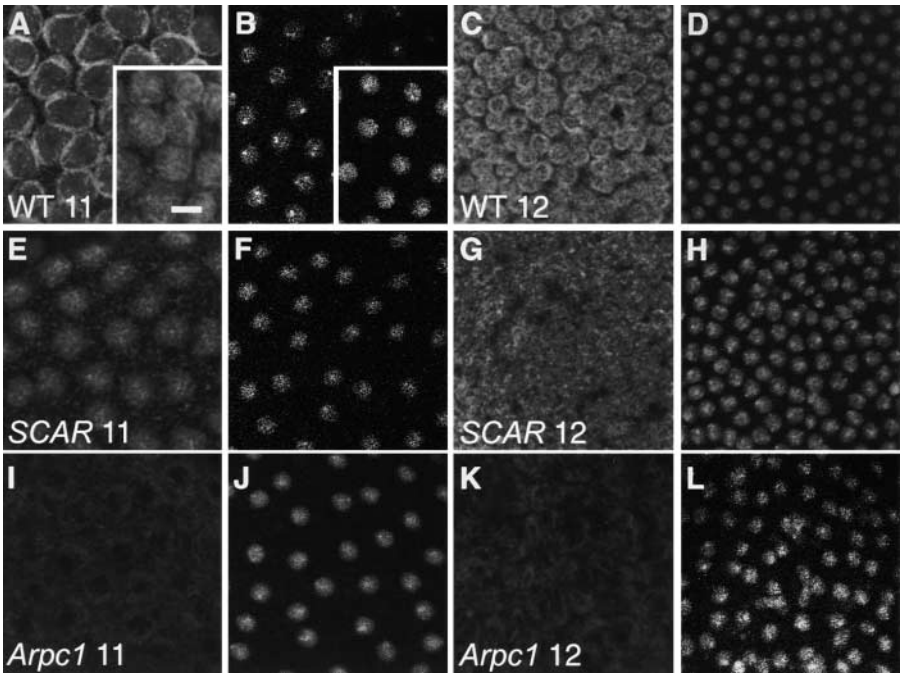

Figure 4. **Interphase actin structures in *SCAR* and *Arpc1* mutant embryos.** Organization of interphase actin caps (first and third columns) and corresponding nuclei (second and fourth columns) are shown. All embryos were fixed, stained, and imaged under identical conditions (except A, inset), allowing for direct comparison. In wild-type embryos (A and C), a cap of actin is present above each nucleus. Wild-type caps are dome shaped, leading to an apparent enrichment of actin at the edges in thick surface views (A and C). In a cycle 11 $SCAR^{mat}$ embryo (E), actin caps appear slightly smaller than in wild-type. $SCAR^{mat}$ actin caps are also flatter than wild-type, resembling a surface-most thinner section of a wild-type cap (A, inset). In a cycle 12 $SCAR^{mat}$ embryo (G), actin caps appear less discrete and are absent in regions above clustered nuclei. In $Arpc1^{mat}$ embryos (I and K), actin is depleted above each nucleus (also Fig. 5 Q). Note that *SCAR* and *Arpc1* consistently display lower levels of fluorescence than wild type. Bar, 10 μm.

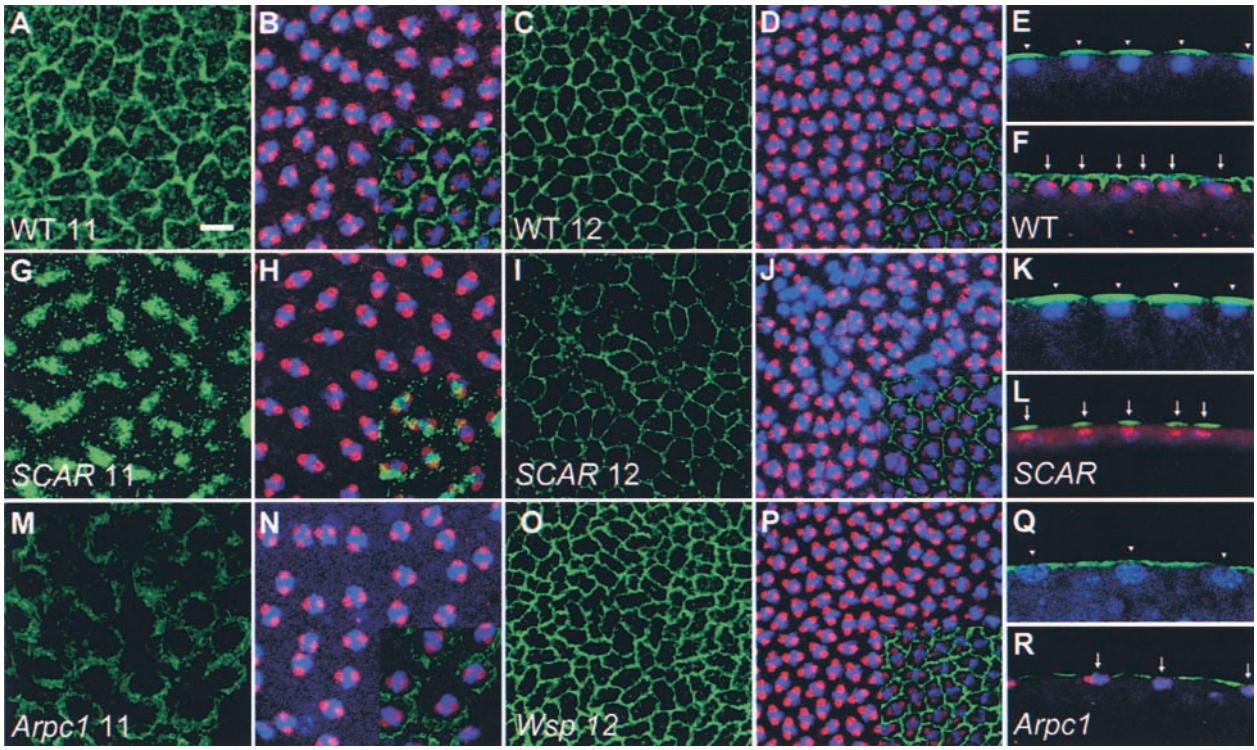

Figure 5. **Metaphase actin furrows are defective in *SCAR* and *Arpc1* embryos.** Filamentous actin structures (phalloidin in green) and mitotic spindles (tubulin in red and DNA in blue) during cycles 11 (columns 1, 2, 5) and 12 (columns 3 and 4). Actin and spindle staining are superimposed in the insets (columns 2 and 4). All embryos are mitotic except E, K, and Q, which are in interphase and not stained for tubulin. Columns 1–4 are surface views, and column 5 shows cross-sections. In a mitotic wild-type cycle 11 (A and B) or 12 (C and D) embryo, actin is present in metaphase furrows between spindles. In cross-section, actin caps lie above each interphase nucleus (E, arrowheads), whereas actin furrows form transient invaginations between mitotic spindles (F, arrows). In a cycle 11 *SCAR*^{mat} embryo (G and H), abnormal surface actin structures overlie individual spindles and fail to form metaphase furrows. In an occasional *SCAR*^{mat} cycle 12 embryo (I and J), a partial metaphase furrow network forms. Cross-sections of *SCAR*^{mat} embryos show actin caps above each interphase nucleus (K, arrowheads) and aberrant actin structures above each mitotic spindle (L, arrows). In an *Arpc1*^{mat} embryo (M and N), actin does not form metaphase furrows and is depleted in the region above each spindle. In contrast, *Wsp*^{mat} embryos form normal metaphase furrows (O and P). Cross-sections of *Arpc1*^{mat} embryos demonstrate actin depletion above interphase nuclei (Q, arrowheads) and mitotic spindles (R, arrows). Bar, 10 μm.

a subset of embryos, primarily in later syncytial divisions 12 and 13, actin caps appeared less discrete and gaps were observed in regions where nuclei were abnormally clustered (Fig. 4 G, 13/35 embryos). In contrast to the relatively mild defects in interphase caps, metaphase furrows were completely absent in the majority of *SCAR*^{mat} embryos undergoing mitosis, and actin accumulated in aberrant structures positioned above rather than between individual spindles (Fig. 5, G, H, and L, 21/28 embryos). A partial and discontinuous metaphase furrow network was observed in a minority of *SCAR*^{mat} embryos (Fig. 5, I and J, and Fig. 2 J, 7/28 embryos). These two mitotic phenotypes were mutually exclusive and consistent across the entire embryo surface. These observations suggest an abnormal reorganization of interphase actin as *SCAR*^{mat} embryos enter mitosis, indicating that the transition between interphase caps and metaphase furrows requires SCAR function.

Major defects in cortical actin structures were also observed in *Arpc1*^{mat} embryos, where interphase actin caps were abnormal and actin appeared to be depleted from the regions above individual nuclei (Fig. 4, I and K, 37/37 embryos). This depletion is apparent most readily in cross-section (Fig. 5 Q). As in *SCAR*, metaphase furrows failed to form in *Arpc1*^{mat} embryos (Fig. 5 M, 12/12 embryos). However, unlike *SCAR*, metaphase actin exhibited a diffuse localization to the broad region between spindles (Fig. 5 R). These results demonstrate that the Arp2/3 complex component Arpc1 is required for the formation of both interphase actin caps and metaphase actin furrows. The greater severity of the *Arpc1* phenotype compared with *SCAR* could reflect a difference in residual gene activity of these partial loss of function alleles.

SCAR and Arpc1, therefore, provide functions that are critical for proper formation of cortical actin structures. In contrast, actin caps and furrows formed normally in *Wsp*^{mat} embryos (27 interphase and 5 metaphase embryos) (Fig. 5, O and P). It is worth emphasizing in this context that both the *SCAR* and *Arpc1* phenotypes result from a partial loss of gene function, whereas early embryogenesis can proceed normally despite complete lack of *Wsp* gene activity.

In addition to defects in organization of microfilament structures, overall actin levels in *Arpc1*^{mat} and *SCAR*^{mat} embryos appeared consistently lower than in wild type. To rigorously assess differences in actin levels, we quantitated surface filamentous actin in syncytial embryos using a phalloidin fluorescence assay. We found that both *Arpc1*^{mat} and *SCAR*^{mat} mutants exhibited significantly reduced levels of surface actin compared with control embryos (Fig. 6). The more severe loss of actin in *Arpc1*^{mat} correlates with the

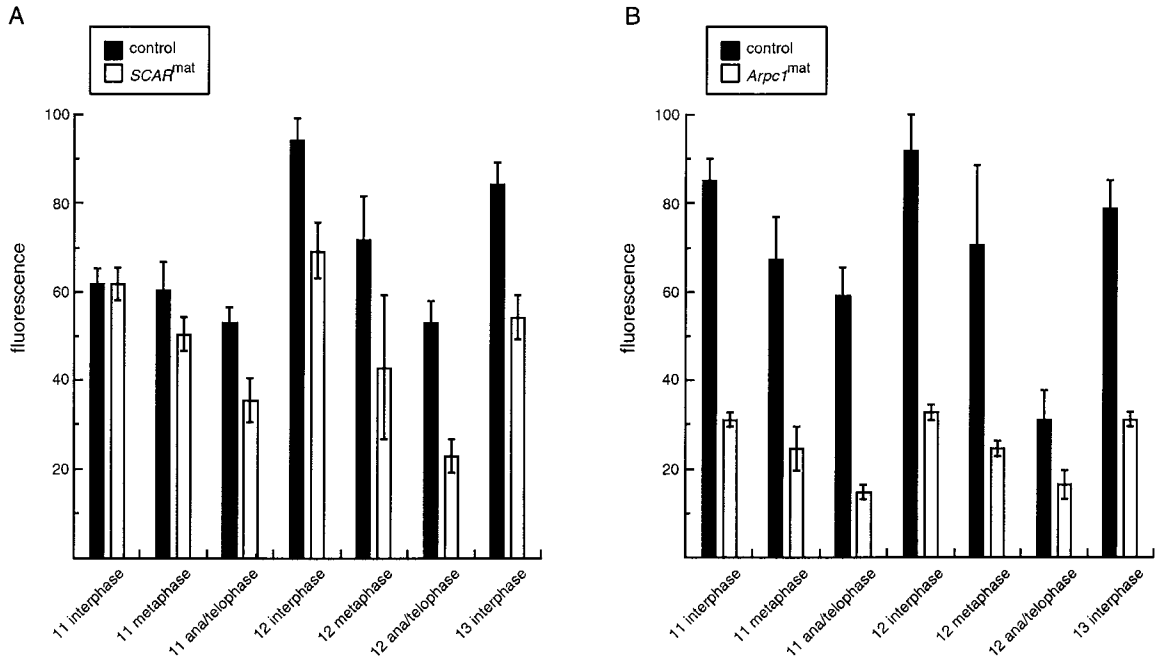

Figure 6. **Reduced filamentous actin in *SCAR* and *Arpc1* mutant embryos.** Fluorescence intensity is indicated in arbitrary units on the y axis. Error bars represent the standard error of the mean and depict the variability between embryos. Embryos were staged according to nuclear morphology (Foe et al., 1993, 2000) and grouped according to syncytial division number and cell cycle stage. To allow for simultaneous staining, embryos derived from *oskar* mutant mothers (Lehmann and Nusslein-Volhard, 1986) served as controls. Such embryos, in which cortical actin structures form normally, are readily distinguished from $SCAR^{mat}$ and $Arpc1^{mat}$ embryos by the absence of pole cells. (A) $SCAR^{mat}$ embryos display comparable actin levels to *oskar* controls at the onset of cycle 11 followed by a reduction in filamentous actin during later syncytial divisions. Control embryos in anaphase and telophase display less actin than at other points in the cell cycle, consistent with previous observations (Foe et al., 2000). 66 $SCAR^{mat}$ and 67 *oskar* embryos were scored. (B) $Arpc1^{mat}$ embryos exhibit a more extreme reduction in actin levels throughout syncytial divisions 11–13. 62 $Arpc1^{mat}$ and 54 *oskar* embryos were scored. Cell cycle–dependent fluctuations in filamentous actin levels persist in $SCAR^{mat}$ and $Arpc1^{mat}$. Similar results were obtained when *SCAR* and *Arpc1* were compared with wild-type Oregon R embryos processed in separate tubes. Combining syncytial stages 10–13 (except ana/telophase), *SCAR* exhibited 56 ± 8% of the wild type 100 ± 6% actin levels (n = 19 $SCAR^{mat}$, 32 Oregon R embryos) and *Arpc1* exhibited 17 ± 4% of the wild type 100 ± 7% actin levels (n = 17 $Arpc1^{mat}$, 24 Oregon R embryos).

greater disruption of actin structures in this mutant. These results indicate that Arpc1 and SCAR are both required for the generation of bulk filamentous actin in the blastoderm and suggest a common basis for the defects in cortical actin structures of *Arpc1* and *SCAR* mutant embryos.

SCAR and Arp2/3 complex components are essential for embryonic CNS axon morphology

The striking enrichment of SCAR expression in the CNS (Fig. 2, E and F) prompted us to examine CNS morphology in *SCAR* mutants using the axon-specific BP102 monoclonal antibody (Fujita et al., 1982). In wild-type embryos, CNS axons travel in two longitudinal bundles that flank the midline and two commissural bundles that cross the midline in each segment (Fig. 7 A). Although no apparent defects were observed in homozygous *SCAR* embryos (Fig. 7, B and I), maternal contribution of *SCAR* transcript or protein may provide sufficient wild-type SCAR activity to mask a functional requirement in the CNS. Partial maternal SCAR function provided by the weak $SCAR^{k13811}$ allele at lower temperature (20–22°C rather than 25°C) is sufficient to produce embryos that develop normally through the blastoderm stages described above, allowing an examination of later CNS development.

Reduction of *SCAR* function achieved in this manner indeed caused dramatic CNS defects (Fig. 7, C and I). The phenotypes observed in these mutants (designated $SCAR^{mat/zyg}$ embryos) required disruption of zygotic *SCAR* function (unpublished data). In $SCAR^{mat/zyg}$ embryos, frequent breaks occurred in longitudinal and commissural bundles (93% of segments, n = 242). In extreme cases, a severe depletion of all axon bundles was observed (Fig. 7 C, 46% of segments). At a lower frequency, $SCAR^{mat/zyg}$ embryos exhibited defects in commissure fasciculation and separation (18% of segments), and medial (13%) or lateral (9%) displacement of axons.

Since SCAR is essential for normal CNS axon morphology, we also examined the zygotic effect of mutations in two members of the Arp2/3 complex, *Arp3* and *Arpc1*. *Arp3* zygotic mutant embryos exhibited a partially penetrant defect in CNS axon morphology with a range of phenotypes that strongly resemble $SCAR^{mat/zyg}$ mutants (Fig. 7, E and J). In particular, the majority of *Arp3* mutants displayed breaks in the longitudinal and commissural axon bundles (Fig. 7 E) (48% of segments in mutant embryos, n = 115 segments). A subset of *Arp3* mutants exhibited defects such as commissure defasciculation or fusion (28% of segments) and medially or laterally displaced axons (3% of segments). *Arp3* heterozygotes also exhibited a low penetrance of axon defects (Fig. 7 J). The CNS morphology of zygotic *Arpc1* single mutants appeared normal, perhaps due to the continued presence of maternal gene products. However, combining zygotic *Arpc1* mutations with an *Arp3*

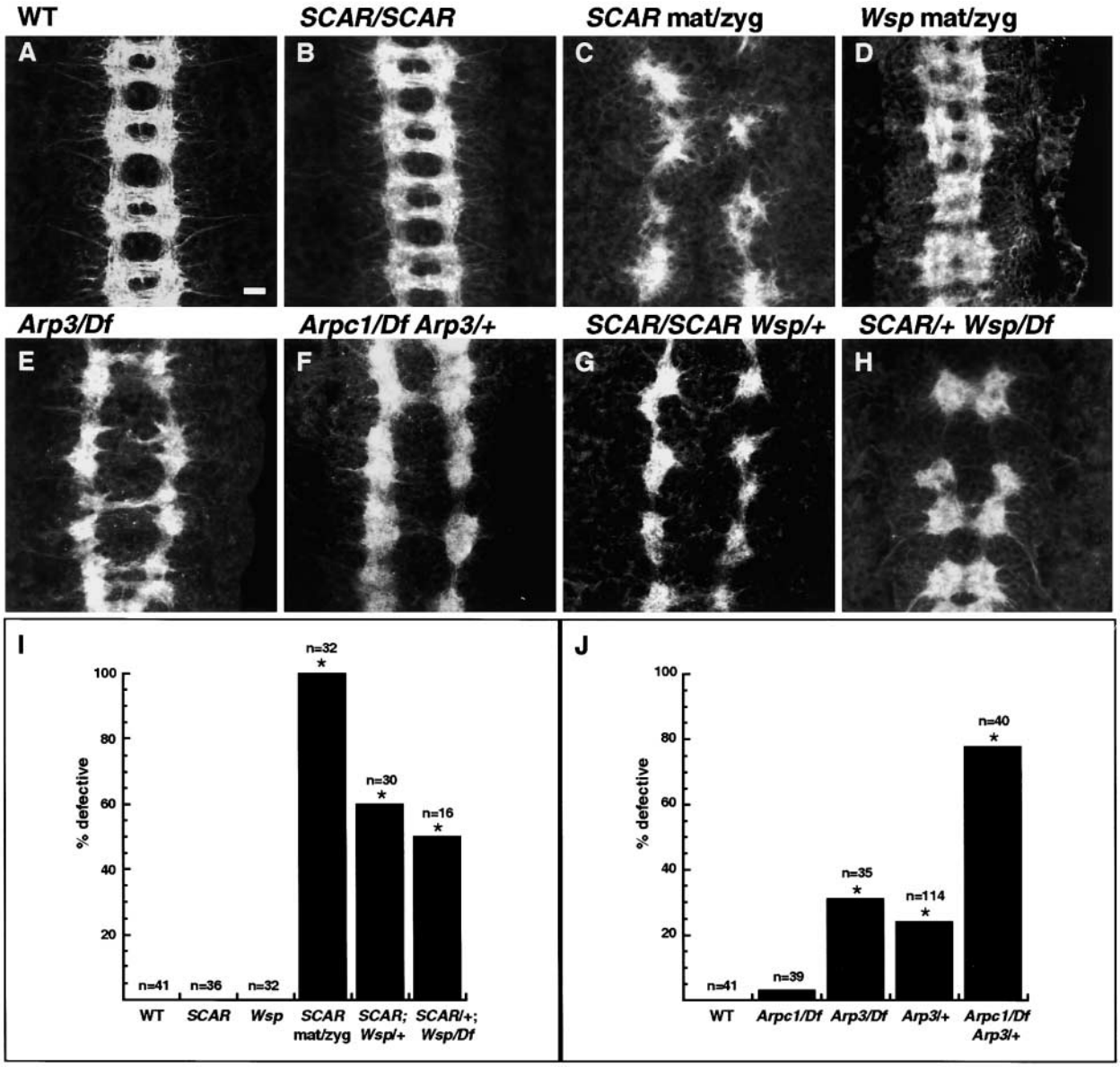

Figure 7. **CNS axon morphology is disrupted by mutations in *SCAR, Wasp*, and the Arp2/3 complex components *Arp3* and *Arpc1*.** CNS axons were visualized with the axon-specific BP102 antibody. (A–H) Ventral view of stage 14/15 embryos; three to four segments in each panel. (A) In wild-type embryos, CNS axons travel in two longitudinal bundles and two commissural bundles in each segment. (B) In a $SCAR^{k13811}$ homozygous mutant embryo, CNS axon morphology appears wild type. $SCAR^{\Delta 37}$ homozygotes were also wild type (unpublished data). (C) In an embryo with reduced maternal and zygotic $SCAR^{k13811}$ function ($SCAR^{mat/zyg}$), gaps appear in both longitudinal and commissural bundles. (D) In an embryo completely lacking maternal and zygotic *Wsp* function ($Wsp^{mat/zyg}$), axon bundles appear thicker and defasciculated; in one segment, axons collapse at the midline. (E) In an *Arp3*/Df(3L)pbl-X1 embryo, breaks in the commissural bundles are observed. (F) In an $Arpc1^{Q25sd}$/Df(2L)b84a9; *Arp3/+* embryo, commissural axons are severely reduced. (G) In a $SCAR^{k13811}/SCAR^{k13811}$; $Wsp^{1}/+$ embryo, there is an apparent depletion of axons in both longitudinal and commissural bundles. (H) In a $SCAR^{k13811}/+$; Wsp^{1}/Df embryo, breaks occur in both longitudinal and commissural axon bundles, and axons are medially displaced. (I and J) Quantitation of CNS axon defects in single and double mutant embryos. The y axis indicates the percentage of embryos with axon defects. n, number of embryos scored (at least 8 segments per embryo). Embryos were scored as mutant if more than half of the segments were defective. Asterisks indicate single mutants that are significantly different from wild-type controls ($p < 0.001$, chi-square test) and double mutants that are significantly different from wild-type and single mutant or heterozygote controls ($p < 0.001$, chi-square test). Bar, 10 μm.

heterozygous background produced defects that were significantly more severe than in *Arp3* heterozygotes alone (Fig. 7, F and J). These phenotypes demonstrate a similar functional requirement for SCAR and Arp2/3 complex components during CNS development.

The contribution of Wasp function to CNS axon morphology is more difficult to assess, since complete removal of maternal and zygotic *Wsp* using the strong Wsp^{3} allele ($Wsp^{mat/zyg}$ embryos) produces cell fate defects in CNS lineages (Ben-Yaacov et al., 2001). An apparent thickening of commissural bundles suggestive of an increase in neuronal number was observed in a majority of $Wsp^{mat/zyg}$ embryos (Fig. 7 D). In addition, most $Wsp^{mat/zyg}$ embryos contained one to two segments with axon bundles collapsed at the midline (Fig. 7 D) (73% of

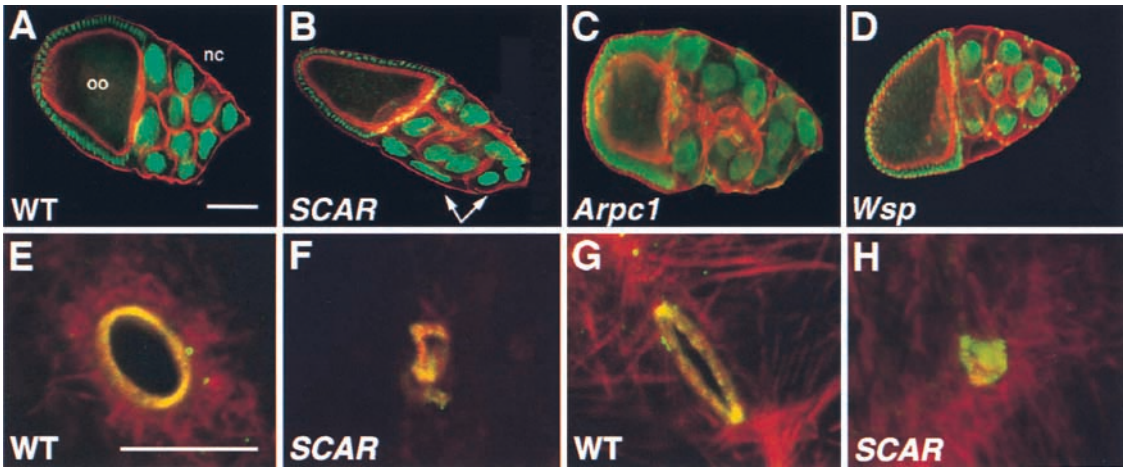

Figure 8. **Abnormal oogenesis in *SCAR* and *Arpc1* mutants.** (A–D) Single egg chambers stained to reveal nuclear arrangement (green, visualized with OliGreen) and nurse cell membranes (red, visualized with phalloidin). (A) Nurse cell (nc) nuclei in a late stage wild-type egg chamber are enclosed in individual cells separated by actin-rich membranes (oo, oocyte). (B) In contrast, a $SCAR^{\Delta 37}$ mutant egg chamber displays a characteristic multinucleate phenotype (arrows). (C) A similar deterioration of egg chamber structure occurs in $Arpc1^{W108R}$ germline clones. (D) Wild-type appearance of a late stage egg chamber from a Wsp^{3} germline clone. (E–H) Ring canals visualized with the Hts-RC antibody (Robinson et al., 1994). Stage 10A (E and F) and 10B (G and H) ring canals are shown. In contrast to the wild-type structures (E and G), $SCAR^{\Delta 37}$ ring canals (F and H) are considerably smaller in size and often occluded. Bars: (A–D) 100 μm; (E–H) 10 μm.

embryos, $n = 41$). Despite these phenotypes, $Wsp^{mat/zyg}$ embryos did not exhibit the severe defects in axon morphology present in *SCAR* and *Arp3* mutants. Although removal of zygotic *SCAR* or *Wsp* function alone did not disrupt CNS morphology (Fig. 7, B and I), zygotic reduction of *SCAR* and *Wsp* together produced significant defects (Fig. 7, G, H, and I) that resemble the strong $SCAR^{mat/zyg}$ phenotype. Therefore, although loss of Wasp function alone does not cause the significant axon defects produced by loss of SCAR, Wasp can influence axon morphology in situations where SCAR function is compromised.

SCAR, and not Wasp, is required with the Arp2/3 complex for egg chamber morphology during oogenesis

Although the partial reduction of SCAR function associated with the $SCAR^{k13811}$ insertion allele is sufficient for normal egg production, the more severe $SCAR^{\Delta 37}$ excision allele produces small and abnormally shaped eggs indicative of a defect in oogenesis. *Drosophila* ovaries house a series of egg chambers that each contain 16 cells (the oocyte and a 15-cell nurse cell complex) interconnected by cytoplasmic bridges (ring canals) that arise from incomplete cytokinesis during mitosis (Spradling, 1993). Morphological defects are apparent in $SCAR^{\Delta 37}$ germline clones during the final phases of oogenesis (Fig. 8). In particular, nurse cells become multinucleate, as many of the actin-lined nurse cell membranes are absent (Fig. 8 B). The morphological abnormalities extend to additional structures, including the actin-rich ring canals, which are significantly smaller than in wild-type and aberrantly shaped (Fig. 8, F and H).

The defects observed in *SCAR* mutant egg chambers closely resemble phenotypes described in mutants for the Arp2/3 complex subunits *Arpc1* and *Arp3* (Hudson and Cooley, 2002), resulting in late stage deterioration of the nurse cell complex (Fig. 8 C). In marked contrast to the *Arpc1*, *Arp3*, and *SCAR* phenotypes, oogenesis in germline clones for the strong loss of function Wsp^{3} allele appears wild type. No apparent morphological abnormalities were observed in Wsp^{3} late stage egg chambers (Fig. 8 D), which can support embryonic development after fertilization (Ben-Yaacov et al., 2001). This phenotypic analysis indicates that SCAR, rather than Wasp, is the major mediator of Arp2/3 function during *Drosophila* oogenesis, much as was observed in the blastoderm and the embryonic CNS.

SCAR and Wasp are required for distinct aspects of Arpc1 function in the adult eye

The above phenotypic analyses identify several Arp2/3-dependent morphological processes that rely on SCAR but are largely independent of Wasp. We therefore asked whether the reciprocal situation exists, namely, are there Arp2/3-mediated events that rely on Wasp but are independent of SCAR? Wasp provides an essential contribution to cell fate decisions in several neural lineages in the *Drosophila* embryo and adult (Ben-Yaacov et al., 2001). Furthermore, the Arp2/3 complex component Arpc1 is required for Wasp-dependent cell fate changes during sensory organ development, and association with Arp2/3 is essential for Wasp function in this context (Tal et al., 2002). This requirement provides an opportunity to examine whether developmental events dependent on Wasp also require SCAR function.

In the adult peripheral nervous system, a primary consequence of mutations in *Wsp* is the excessive differentiation of sensory organ neurons at the expense of nonneuronal cell types, resulting in a marked absence of mechanosensory bristles (Fig. 9, A and B). We used the *ey*-FLP-FRT system (Newsome et al., 2000) to generate mosaic *SCAR* and *Arpc1* heterozygous flies in which head capsule structures and cuticle are derived from homozygous mutant clones induced in the eye imaginal disc. *Arpc1* mosaic heads like, *Wsp*, display a pronounced bristle loss phenotype (Fig. 9 C), which results from cell fate defects similar to those present in *Wsp*

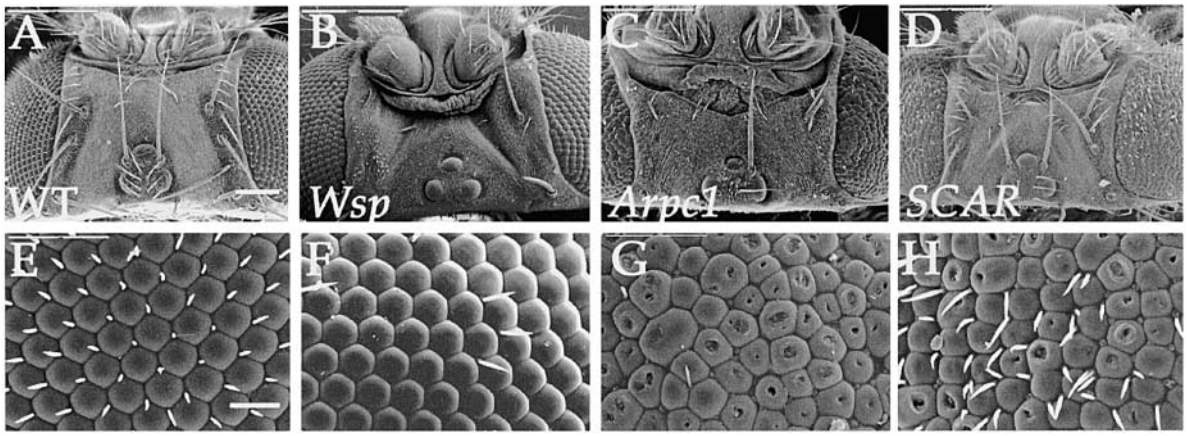

Figure 9. **Distinct head bristle patterns and eye morphologies of *Wsp, Arpc1, and SCAR* mutants.** Scanning electron microscope images of head cuticle (A–D) and enlarged portions of compound eyes (E–H). Nearly all bristles present on the dorsal aspect of the head and the interommatidial bristles of the eye in wild type (A) are missing in a Wsp^{1}/Df(3R)3450 mutant (B). Extensive bristle loss and a rough-eye phenotype are apparent in an $Arpc1^{Q25sd}$ mosaic head (C). The bristle pattern of a $SCAR^{\Delta 37}$ mosaic (D) appears wild type, whereas the eye facet arrangement is abnormal. The enlargement in E shows a highly symmetrical organization of ommatidia and interommatidial bristles in a wild-type eye. A Wsp^{1}/Df(3R)3450 eye (F) exhibits a normal ommatidial array and a pronounced lack of bristles. The abnormal eye facet pattern of a $Arpc1^{Q25sd}$ mosaic eye (G) is characterized by irregularly shaped ommatidia, craters of missing lens material, and a bristle-loss phenotype. A $SCAR^{\Delta 37}$ mosaic eye (H) shows similar morphological defects, but a considerable number of interommatidial bristles are present. Bars: (A–D) 100 μm; (E–H) 25 μm.

mutants (Tal et al., 2002). In contrast, the sensory organ pattern in mosaic heads of strong *SCAR* alleles appears wild type (Fig. 9 D), suggesting that SCAR does not play an essential role in lineage decisions mediated by Wasp and the Arp2/3 complex.

In addition to loss of sensory organ structures, *Arpc1* mosaics display abnormalities in eye structure, including a reduction in the overall size of the eye, irregularly shaped ommatidia, and a distinct loss of lens material in most eye facets (Fig. 9, C and G). Mosaics for the $SCAR^{\Delta 37}$ excision allele present a very similar eye phenotype (Fig. 9, D and H), with the exception that interommatidial bristles are largely present. As noted previously (Ben-Yaacov et al., 2001), mutations in *Wsp* have no discernible effect on eye morphology apart from the bristle loss phenotype (Fig. 9, B and F). This analysis provides a striking example of the distinct requirements for SCAR and Wasp, which mediate separate aspects of Arp2/3 complex function during adult development.

Discussion

These results present the first genetic analysis of Scar function in a multicellular organism and demonstrate a requirement for Scar and the Arp2/3 complex in regulating the morphology of multiple cell types. The highly similar requirements for *Drosophila* SCAR and Arp2/3 complex components in regulating cytoplasmic organization in the blastoderm and cell morphology in CNS neurons, egg chambers, and adult eyes suggest that they function in a common pathway in vivo, consistent with their well-established regulatory interaction in vitro. These roles of SCAR and the Arp2/3 complex are largely independent of Wasp function, suggesting that SCAR is the primary regulator of Arp2/3-dependent morphological processes in *Drosophila*. In contrast, Wasp is specifically required for the Arp2/3-dependent regulation of asymmetric cell divisions (Ben-Yaacov et al., 2001; Tal et al., 2002) a process that is independent of SCAR (this study). These results demonstrate that SCAR and Wasp perform generally nonoverlapping functions during *Drosophila* development and that the Arp2/3 complex can participate in distinct cell biological events in response to different regulators. Although SCAR and Wasp can account for all characterized Arp2/3 complex functions in *Drosophila*, recent studies have described Arp2/3 complex regulators outside of the Scar/Wasp family (Jeng and Welch, 2001). Therefore, homologs of such elements (such as Cortactin and Eps15/Pan1p) may also play a role in Arp2/3-dependent processes during *Drosophila* development.

SCAR is a key regulator of CNS axon morphology

Here we demonstrate a requirement for SCAR in the regulation of axon morphology in the *Drosophila* CNS. The striking enrichment of SCAR protein in axons is consistent with a direct role for SCAR in axon development. In particular, the breaks in longitudinal and commissural axon bundles in *SCAR* mutant embryos may indicate a defect in axon growth. However, these phenotypes could also reflect defects in other aspects of nervous system formation, such as axon guidance, axon initiation, or neuronal differentiation. Morphological characterization of *SCAR* mutants at single neuron resolution will provide greater insight into the processes that require SCAR function.

The CNS axon defects in *SCAR* mutant embryos resemble defects caused by simultaneous zygotic disruption of the Abl tyrosine kinase and a diverse set of elements including the Fasciclin I transmembrane protein, Armadillo/β-catenin, Chickadee/profilin, and the Trio Rac/Rho guanine nucleotide exchange factor (Lanier and Gertler, 2000). Interestingly, Scar/WAVE-1 has been shown to associate with the SH3 domain of the Abl tyrosine kinase, suggesting that they may directly interact in vivo (Westphal et al., 2000). The observation that multiple zygotic

mutations are required to replicate the *SCAR* phenotype is consistent with a model where SCAR functions downstream of multiple signaling pathways that converge on regulation of the actin cytoskeleton.

The defects in axon morphology caused by reduction of maternal and zygotic SCAR are similar to those produced by zygotic disruption of Arp3 or simultaneous zygotic disruption of Arp3 and Arpc1 or SCAR and Wasp. These results suggest that SCAR, Wasp, and the Arp2/3 complex may affect a common process in neuronal development involving actin regulation. The contribution of both SCAR and Wasp to axon morphology could be explained by several possible mechanisms. In one model, SCAR and Wasp might regulate a common activity of the Arp2/3 complex, such as in the context of a specific actin structure or in contribution to bulk actin levels. Their functional differences in vivo could be achieved through differences in expression, activation, or subcellular localization. Alternatively, SCAR and Wasp could regulate distinct activities of the Arp2/3 complex, producing different actin structures that participate in diverse cell biological processes such as cell morphology (SCAR) and asymmetric cell division (Wasp). It will be interesting to examine how SCAR and Wasp intersect with regulators and effectors to achieve the specific organization of actin structures in different contexts.

SCAR and the Arp2/3 complex regulate actin polymerization and organization in the blastoderm embryo

The dramatic reduction in actin levels of *Drosophila Arpc1* mutants indicates that the Arp2/3 complex is an essential source of filamentous actin in the blastoderm embryo. This is consistent with experiments in other systems, where the Arp2/3 complex is required for actin polymerization in yeast actin patches (Pelham and Chang, 2001) and cell extracts in response to the Cdc42 GTPase (Ma et al., 1998; Mullins and Pollard, 1999) or the *Listeria* pathogen (Welch et al., 1997). Our results also suggest that the SCAR regulator mediates this Arp2/3-dependent actin polymerization in the blastoderm. A similar reduction in filamentous actin is observed in *Dictyostelium* Scar mutants (Bear et al., 1998), and budding yeast Bee1 is required for actin polymerization at actin patch structures in a permeabilized cell assay (Lechler and Li, 1997). Together, these results demonstrate a conserved role for the Arp2/3 complex and WASp/Scar proteins in promoting actin polymerization in vivo as well as in vitro.

In budding and fission yeast, inducible disruption of Arp2/3 complex function first leads to a cessation of actin patch movement followed by their eventual dissolution (Winter et al., 1997; Pelham and Chang, 2001). Therefore, the Arp2/3 complex is required for the motility of actin structures and their formation. Similarly, *Dictyostelium* Scar mutants exhibit a selective disruption of specific actin structures that cannot easily be explained by an overall reduction of actin. Actin correctly localizes to the cell cortex and extending pseudopods as in wild type; however, leading edge actin fails to coalesce in response to chemoattractant, often leading to the aberrant formation of multiple pseudopods (Bear et al., 1998). These results suggest that Scar is involved in the dynamic organization of actin structures as well as their generation.

An exciting possibility is that Scar and the Arp2/3 complex direct both the configuration and polymerization of actin in the *Drosophila* blastoderm. *SCAR* embryos in metaphase contain more than half the actin of wild-type embryos, yet this substantial amount of actin often fails to form even a discontinuous network of metaphase furrows. Instead, actin remains in aberrant surface structures that are not normally found at the surface of mitotic embryos. These observations suggest that SCAR plays a role in actin redistribution, perhaps through a local Arp2/3-dependent polymerization event that triggers a global cell cycle–dependent change in actin organization. This role of SCAR in the *Drosophila* embryo may be analogous to the reorganization of actin structures that occurs in other contexts, such as during cytokinesis or at the leading edge of migrating cells.

Materials and methods

Fly stocks and genetics

Flies were maintained using standard methods. Wild-type stocks were Oregon R (immunohistochemistry) and *oskar*^{166} (SCAR antibody controls and actin quantitation) (Lehmann and Nusslein-Volhard, 1986). See Flybase (http://flybase.bio.indiana.edu) for details concerning fly stocks. Alleles used were *Arp3*$^{EP(3)3640}$ (Rørth, 1996; Berkeley *Drosophila* Genome Project), *Wsp*^{1}, *Wsp*^{3} (Ben-Yaacov et al., 2001), *Arpc1*^{R337st}, *Arpc1*^{Q25sd}, *Arpc1*^{W108R} (Hudson and Cooley, 2002), *SCAR*^{k13811} (Spradling et al., 1999; Berkeley *Drosophila* Genome Project), and *SCAR*$^{\Delta 37}$.

Germline clones were generated as described (Chou and Perrimon, 1996) by heat shock of *hs-FLP*; *ovoD* FRT40A/*SCAR* FRT40A larvae, *hs-FLP*; FRT82B *ovoD*/FRT82B *Wsp* larvae, or *hs-FLP*; *ovoD* FRT40A/*Arpc1* FRT40A larvae. Adult germline clone females were mated to Oregon R males (blastoderm and oogenesis analysis) or to *SCAR*^{k13811}/CyO en-lacZ males (*SCAR*$^{mat/zyg}$) or Df(3R)3450/TM6B abdA-lacZ males (*Wsp*$^{mat/zyg}$) (CNS). Mosaic head clones were obtained in *ey*-FLP; *Arpc1*^{Q25sd} FRT40A/l(2)cl-L3^{1} FRT40A and *ey*-FLP; *SCAR*$^{\Delta 37}$ FRT40A/l(2)cl-L3^{1} FRT40A flies. *SCAR*^{k13811} and *Wsp*^{3} germline clones (blastoderm), *Wsp*^{3} germline clones (CNS), and all zygotic mutants were generated at 25°C. *Arpc1*^{R337st} germline clones (blastoderm) and *SCAR*^{k13811} germline clones (CNS) were generated at 20–22°C.

We observed no contribution of zygotic gene activity to the blastoderm defects of embryos derived from *SCAR*^{k13811} and *Arpc1*^{R337st} germline clones (unpublished data). *Wsp*^{mat} embryos include embryos defective for both maternal and zygotic *Wsp* function and embryos defective only for maternal *Wsp* function.

cDNA expression

The full-length *SCAR* cDNA from the SD02991 EST was cloned as an EcoRV-XhoI (blunt) fragment into the pUASP vector (Rørth, 1998). Transgenic flies containing the UAS-*SCAR* transgene were generated by P-element–mediated transformation and two independent lines used for phenotypic rescue. Rescue to adult viability was obtained in *SCAR*/*SCAR*; UAS-SCAR/P{tubP-GAL4} for *SCAR*^{k13811} and *SCAR*$^{\Delta 37}$ homozygotes.

SCAR antibody generation

The SCAR NH_2-terminal region (amino acids 1–237) was cloned into the pRSET vector (Invitrogen) to generate a 6×His-tagged protein, which was purified and injected into guinea pigs (Cocalico Biologicals). SCAR polyclonal antibody was used at a 1:50 dilution to stain formaldehyde-fixed embryos as described (Theurkauf, 1994). SCAR polyclonal antibody was visualized with Alexa 546–conjugated secondary antibody and costained with Alexa 488–conjugated phalloidin (Molecular Probes).

P-element excision

The *l(2)k13811* P-element insertion in the 5′ UTR of *SCAR* was mobilized by introducing transposase on the chromosome CyO Δ2-3. Excisions were identified in F2 progeny derived from single males of the genotype w; *SCAR*^{k13811}/CyO Δ2-3. 15 homozygous viable alleles complemented the *SCAR*^{k13811} lethality and are likely to represent precise excision events, verified by sequencing one such chromosome. 11 (presumably imprecise) excision alleles failed to complement the *SCAR*^{k13811} lethality and were homozygous lethal. The *Δ37* excision allele complements the lethality of *l(2)06225*, an insertion within the CG6105 transcription unit 400 bp up-

stream of *SCAR* (Fig. 1 A) and fails to complement the sterility of the downstream *piwi* gene.

Single larva PCR

SCAR$^{\Delta 37}$ homozygotes were chosen as nonfluorescing larvae from a *SCAR*$^{\Delta 37}$/CyO, Act-GFP stock. Genomic DNA was prepared from five individual larvae, and PCR amplification for sequencing was performed using primers from the *SCAR* region.

CNS axon morphology

Embryos were fixed for 20 min in 3.7% formaldehyde/PBS:heptane and devitellinized in heptane:methanol. Embryos were stained with mouse mAb BP102 (1:10 dilution; Developmental Studies Hybridoma Bank) and rabbit anti–β-galactosidase (1:1,500 dilution; Cappel), followed by fluorescence-conjugated Alexa 488 and Alexa 546 secondary antibodies (Molecular Probes), and mounted in Aquapolymount (Polysciences, Inc.). Images were z-series projections obtained on a ZEISS LSM 510 confocal microscope. CyO en-lacZ, TM6B abdA-lacZ, and TM3 Ubx-lacZ balancers were used to genotype embryos. For *Arp3* heterozygotes, *Arp3*/balancer females were mated to WT males. When deficiencies were used, mutant/balancer females were mated to deficiency/balancer males. For double mutant analyses, double mutant females were crossed to deficiency/balancer or *SCAR*^{k13811}/balancer males. Statistics were computed using the Primer of Biostatistics program (Stanton Glantz) and Numerical Recipes in C (Press et al., 1992).

Actin quantitation

Embryos were collected at 20–22°C (*Arpc1*^{mat} and *oskar* control) or 25°C (*SCAR*^{mat} and *oskar* control), fixed for 45 min in 19% formaldehyde/PBS: heptane, and hand devitellinized. Control and mutant embryos were pooled and incubated in a single tube for 2 h with 6.6 nM Alexa 488–conjugated phalloidin (Molecular Probes) and 0.1 μg/ml Hoechst (Sigma-Aldrich). Mean surface fluorescence intensity was measured for two areas of each embryo (the brightest surface 1.5 μm optical slice) and averaged. Images were obtained on a ZEISS LSM 510 confocal microscope using a C-Apochromatic 40×/1.2 NA water immersion objective. Images were generated using identical linear gain settings at zoom 3 and 1,024 pixel^2 resolution to achieve Nyquist resolution, an optimal sampling rate. Gain settings were determined empirically to allow a range of intensities to be detected with minimal saturation of the higher control signal. Fluorescence intensity was quantitated in ImagePro Plus (Media Cybernetics). Background fluorescence was determined from 15 embryos processed identically but without phalloidin; these embryos displayed a nearly identical nonzero fluorescence, which was subtracted from the measured fluorescence in all images. Standard error of the mean was calculated in Kaleidagraph. In separate experiments to assess actin distribution (Fig. 5), embryos were costained with mouse anti–β-tubulin antibodies (1:500 dilution; Sigma-Aldrich) for precise cell cycle staging. Antibody staining obscured the difference in phalloidin fluorescence; therefore, no antibodies were included in the quantitation experiment.

Egg chamber morphology

Ovaries were dissected from 3–5 d-old females and fixed for 15 min in 6% formaldehyde/PBS. Germline clones could first be identified after stage 8 of oogenesis (Spradling, 1993). Egg chamber microfilaments were visualized by staining with rhodamine-phalloidin (1 U/ml, 20 min; Molecular Probes), nuclei with OliGreen (1:5,000, 10 min, after a 1-h treatment with 5 μg/ml RNase; Molecular Probes), and ring canals with monoclonal Hts-RC antibody (clone 7C, 1:10 dilution).

SEM analysis of head cuticle and eye phenotypes

Adult heads underwent critical point drying and sputter coating with a gold film after dehydration in an ethanol series. Scanning EM was performed using a JEOL JSM-6400 microscope.

We are grateful to Joe Goodhouse for assistance with confocal microscopy, Bahram Houchmandzadeh for advice on statistical analysis, and Eugenia Klein for instruction and skillful operation of the scanning electron microscope. We thank Mimi Shirasu-Hiza, Rachel Hoang, Jörg Großhans, Ali Nouri, Cheryl Van Buskirk, and anonymous reviewers for helpful comments on the article. Some stocks were obtained from the Bloomington *Drosophila* Stock Center.

J.A. Zallen was supported by a Koshland Postdoctoral Fellowship and is a Postdoctoral Fellow of the Damon Runyon-Walter Winchell Foundation Cancer Research Fund. E. Wieschaus is an Investigator of the Howard Hughes Medical Institute. E.D. Schejter is supported by grants from the Israel Science Foundation and the Minerva Foundation.

Submitted: 18 September 2001
Revised: 11 January 2002
Accepted: 14 January 2002

References

Bear, J.E., J.F. Rawls, and C.L. Saxe, III. 1998. SCAR, a WASP-related protein isolated as a suppressor of receptor defects in late *Dictyostelium* development. *J. Cell Biol.* 142:1325–1335.

Ben-Yaacov, S., R. Le Borgne, I. Abramson, F. Schweisguth, and E.D. Schejter. 2001. Wasp, the *Drosophila* Wiskott-Aldrich syndrome gene homologue, is required for cell fate decisions mediated by Notch signaling. *J. Cell Biol.* 152:1–13.

Borisy, G.G., and T.M. Svitkina. 2000. Actin machinery: pushing the envelope. *Curr. Opin. Cell Biol.* 12:104–112.

Chou, T.B., and N. Perrimon. 1996. The autosomal FLP-DFS technique for generating germline mosaics in *Drosophila melanogaster*. *Genetics.* 144:1673–1679.

Cox, D.N., A. Chao, J. Baker, L. Chang, D. Qiao, and H. Lin. 1998. A novel class of evolutionarily conserved genes defined by *piwi* are essential for stem cell self-renewal. *Genes Dev.* 12:3715–3727.

Cox, D.N., A. Chao, and H. Lin. 2000. *piwi* encodes a nucleoplasmic factor whose activity modulates the number and division rate of germline stem cells. *Development*. 127:503–514.

Dramsi, S., and P. Cossart. 1998. Intracellular pathogens and the actin cytoskeleton. *Annu. Rev. Cell Dev. Biol.* 14:137–166.

Fawcett, J., and T. Pawson. 2000. Signal transduction. N-WASP regulation—the sting in the tail. *Science.* 290:725–726.

Foe, V.E., G.M. Odell, and B.A. Edgar. 1993. Mitosis and morphogenesis in the *Drosophila* embryo: point and counterpoint. *In* The Development of *Drosophila melanogaster.* M. Bate and A. Martinez-Arias, editors. Cold Spring Harbor Laboratory Press, Cold Spring Harbor, NY. 149–300.

Foe, V.E., C.M. Field, and G.M. Odell. 2000. Microtubules and mitotic cycle phase modulate spatiotemporal distributions of F-actin and myosin II in *Drosophila* syncytial blastoderm embryos. *Development.* 127:1767–1787.

Fujita, S.C., S.L. Zipursky, S. Benzer, A. Ferrus, and S.L. Shotwell. 1982. Monoclonal antibodies against the *Drosophila* nervous system. *Proc. Natl. Acad. Sci. USA.* 79:7929–7933.

Fyrberg, C., L. Ryan, M. Kenton, and E. Fyrberg. 1994. Genes encoding actin-related proteins of *Drosophila melanogaster*. *J. Mol. Biol.* 241:498–503.

Goldstein, L.S., and S. Gunawardena. 2000. Flying through the *Drosophila* cytoskeletal genome. *J. Cell Biol.* 150:F63–F68.

Higgs, H.N., and T.D. Pollard. 2001. Regulation of actin filament network formation through Arp2/3 complex: activation by a diverse array of proteins. *Annu. Rev. Biochem.* 70:649–676.

Hudson, A.M., and L. Cooley. 2002. A subset of dynamic actin rearrangements in *Drosophila* requires the Arp2/3 complex. *J. Cell Biol.* 156:677–687.

Jeng, R.L., and M.D. Welch. 2001. Actin and endocytosis—no longer the weakest link. *Curr. Biol.* 11:R691–R694.

Karr, T.L., and B.M. Alberts. 1986. Organization of the cytoskeleton in early *Drosophila* embryos. *J. Cell Biol.* 102:1494–1509.

Lanier, L.M., and F.B. Gertler. 2000. From Abl to actin: Abl tyrosine kinase and associated proteins in growth cone motility. *Curr. Opin. Neurobiol.* 10:80–87.

Lechler, T., and R. Li. 1997. In vitro reconstitution of cortical actin assembly sites in budding yeast. *J. Cell Biol.* 138:95–103.

Lehmann, R., and C. Nusslein-Volhard. 1986. Abdominal segmentation, pole cell formation, and embryonic polarity require the localized activity of oskar, a maternal gene in *Drosophila. Cell.* 47:141–152.

Li, R. 1997. Bee1, a yeast protein with homology to Wiscott-Aldrich Syndrome protein, is critical for the assembly of cortical actin cytoskeleton. *J. Cell Biol.* 136:649–658.

Ma, L., R. Rohatgi, and M.W. Kirschner. 1998. The Arp2/3 complex mediates actin polymerization induced by the small GTP-binding protein Cdc42. *Proc. Natl. Acad. Sci. USA.* 95:15362–15367.

Machesky, L.M., and K.L. Gould. 1999. The Arp2/3 complex: a multifunctional actin organizer. *Curr. Opin. Cell Biol.* 11:117–121.

May, R.C. 2001. The Arp2/3 complex: a central regulator of the actin cytoskeleton. *Cell. Mol. Life Sci.* 58:1607–1626.

Mullins, R.D., and T.D. Pollard. 1999. Rho-family GTPases require the Arp2/3 complex to stimulate actin polymerization in *Acanthamoeba* extracts. *Curr. Biol.* 9:405–415.

Mullins, R.D., J.A. Heuser, and T.D. Pollard. 1998. The interaction of Arp2/3 complex with actin: nucleation, high affinity pointed end capping, and formation of branching networks of filaments. *Proc. Natl. Acad. Sci. USA.* 95: 6181–6186.

Naqvi, S.N., R. Zahn, D.A. Mitchell, B.J. Stevenson, and A.L. Munn. 1998. The WASp homologue Las17p functions with the WIP homologue End5p/verprolin and is essential for endocytosis in yeast. *Curr. Biol.* 8:959–962.

Newsome, T.P., B. Asling, and B.J. Dickson. 2000. Analysis of *Drosophila* photoreceptor axon guidance in eye-specific mosaics. *Development.* 127:851–860.

Pantaloni, D., C. Le Clainche, and M.F. Carlier. 2001. Mechanism of actin-based motility. *Science.* 292:1502–1506.

Pelham, R.J., Jr., and F. Chang. 2001. Role of actin polymerization and actin cables in actin-patch movement in *Schizosaccharomyces pombe. Nat. Cell Biol.* 3:235–244.

Press, W.H., S.A. Teukolsky, W.T. Vetterling, and B.P. Flannery. 1992. Numerical recipes in C. Cambridge University Press, Cambridge, UK. 1020 pp.

Qualmann, B., M.M. Kessels, and R.B. Kelly. 2000. Molecular links between endocytosis and the actin cytoskeleton. *J. Cell Biol.* 150:F111–F116.

Robinson, D.N., K. Cant, and L. Cooley. 1994. Morphogenesis of *Drosophila* ovarian ring canals. *Development.* 120:2015–2025.

Rørth, P. 1996. A modular misexpression screen in *Drosophila* detecting tissue-specific phenotypes. *Proc. Natl. Acad. Sci. USA.* 93:12418–12422.

Rørth, P. 1998. Gal4 in the *Drosophila* female germline. *Mech. Dev.* 78:113–118.

Rubin, G.M., L. Hong, P. Brokstein, M. Evans-Holm, E. Frise, M. Stapleton, and D.A. Harvey. 2000. A *Drosophila* complementary DNA resource. *Science.* 287:2222–2224.

Schejter, E.D., and E. Wieschaus. 1993. Functional elements of the cytoskeleton in the early *Drosophila* embryo. *Annu. Rev. Cell Biol.* 9:67–99.

Spradling, A. 1993. Developmental genetics of oogenesis. *In* The Development of *Drosophila melanogaster*. M. Bate and A. Martinez-Arias, editors. Cold Spring Harbor Laboratory Press, Cold Spring Harbor, NY. 1–70.

Spradling, A.C., D. Stern, A. Beaton, E.J. Rhem, T. Laverty, N. Mozden, S. Misra, and G.M. Rubin. 1999. The Berkeley *Drosophila* Genome Project gene disruption project. Single P-element insertions mutating 25% of vital *Drosophila* genes. *Genetics*. 153:135–177.

Takenawa, T., and H. Miki. 2001. WASP and WAVE family proteins: key molecules for rapid rearrangement of cortical actin filaments and cell movement. *J. Cell Sci.* 114:1801–1809.

Tal, T., D. Vaizel-Ohayon, and E.D. Schejter. 2002. Conserved interactions with cytoskeletal but not signaling elements are an essential aspect of *Drosophila* Wasp function. *Dev. Biol.* In press.

Taunton, J. 2001. Actin filament nucleation by endosomes, lysosomes and secretory vesicles. *Curr. Opin. Cell Biol.* 13:85–91.

Theurkauf, W.E. 1994. Immunofluorescence analysis of the cytoskeleton during oogenesis and early embryogenesis. *Methods Cell Biol.* 44:489–505.

Welch, M.D., A. Iwamatsu, and T.J. Mitchison. 1997. Actin polymerization is induced by Arp2/3 protein complex at the surface of *Listeria monocytogenes. Nature.* 385:265–269.

Welch, M.D., J. Rosenblatt, J. Skoble, D.A. Portnoy, and T.J. Mitchison. 1998. Interaction of human Arp2/3 complex and the *Listeria monocytogenes* ActA protein in actin filament nucleation. *Science.* 281:105–108.

Westphal, R.S., S.H. Soderling, N.M. Alto, L.K. Langeberg, and J.D. Scott. 2000. Scar/WAVE-1, a Wiskott-Aldrich syndrome protein, assembles an actin-associated multi-kinase scaffold. *EMBO J.* 19:4589–4600.

Winter, D., A.V. Podtelejnikov, M. Mann, and R. Li. 1997. The complex containing actin-related proteins Arp2 and Arp3 is required for the motility and integrity of yeast actin patches. *Curr. Biol.* 7:519–529.

Winter, D.C., E.Y. Choe, and R. Li. 1999. Genetic dissection of the budding yeast Arp2/3 complex: a comparison of the in vivo and structural roles of individual subunits. *Proc. Natl. Acad. Sci. USA.* 96:7288–7293.

Zalokar, M., and I. Erk. 1976. Division and migration of nuclei during early embryogenesis of *Drosophila melanogaster. J. Microsc. Biol. Cell.* 25:97–106.